Composites Science and Technology 136 (2016) 29–38

Contents lists available at ScienceDirect

Composites Science and Technology

journal homepage: http://www.elsevier.com/locate/compscitech

MWCNT based matrices as a platform for adhesion and growth of cells

Alicja Warowicka [a, **, 1], Barbara M. Maciejewska [a, *, 1], Jagoda Litowczenko [a], Mikołaj Kościński [a, b], Anna Baranowka-Korczyc [a], Małgorzata Jasiurkowska-Delaporte [a], Krzysztof K. Koziol [d], Stefan Jurga [a, c]

[a] NanoBioMedical Centre, Adam Mickiewicz University, ul. Umultowska 85, PL-61614 Poznań, Poland
[b] Life Sciences University, Department of Physics, PL-60637 Poznań, Wojska Polskiego 38/42, Poland
[c] Department of Macromolecular Physics, Faculty of Physics, Adam Mickiewicz University, Umultowska 85, PL-61614 Poznań, Poland
[d] University of Cambridge, Department of Materials Science and Metallurgy, 27 Charles Babbage Road, Cambridge CB3 0FS, UK

ARTICLE INFO

Article history:
Received 1 August 2016
Received in revised form
28 September 2016
Accepted 30 September 2016
Available online 1 October 2016

Keywords:
Carbon nanotubes
Chemical vapour deposition (CVD)
Surface treatments
Annealing
Cell growth

ABSTRACT

In this study we examine multiwall carbon nanotube (MWCNT) based nanosystems i.e. aligned MWCNT matrices, as potential scaffolds for cell growth and tissue engineering. We present the effect of samples purification and surface modification on the viability, adhesiveness and morphology of human normal gingival fibroblasts (HGF-1) and human osteosarcoma (U2OS) cell lines. We employ spectroscopic and analytical techniques (Scanning Electron Microscopy, Thermal Gravimetric Analysis, Atomic Force Microscopy, Raman and Fourier Transform Infrared Absorption Spectroscopy and Confocal Microscopy) in order to characterize the obtained structures. Furthermore, we analyze the expression level of selected cell adhesion-related genes by the quantitative real-time (qRT-PCR) method and the cell viability for MWCNT powders. We show that the surface structure of MWCNTs carpets contributes to the adhesion of cells. Additionally, we report the increased expression level of integrin, talin and fibronectin, proteins which are involved in cell attachment. We speculate that carbon nanotube based materials can be consider as potential candidates for biomedical purposes and as a biocompatible scaffold for cell growth.

1. Introduction

New nanomaterials for tissue engineering applications are highly demanded and still drive much attention. One of major approaches in this area, and in regenerative medicine, is the application of carbon-based nanomaterials, including graphene and carbon nanotubes, in different shapes and forms. Several types of carbon-based matrices have been proposed so far i.e. MWCNTs platform based on polymer, ones with specified cavities size, carbon based nanocomposites [1]. MWCNTs dispersed in polymer matrixes, aligned MWCNTs [2] and many others. The main reason to implement carbon nanostructures into scaffolds is to improve the mechanical properties by increasing the Young modulus and tensile strength of the structure. Furthermore, the combination of carbon nanomaterials with substrates support cell attachment, growth and differentiation [3]. Moreover, carbon nanomaterials can be biologically functionalized with various molecules to design scaffolds for tissue growth [4,5]. CNTs show a high binding affinity to biomolecules, including extracellular matrix (ECM) proteins, e.g fibronectin. Interestingly, authors proposed fibronectin – carbon nanotubes composite (hybrid nanostructure) as a pattern (matrix) for controlled cell adhesion and growth of various cells [6,7].

Recently, the interactions of CNTs with cells have been studied, for example adhesion, morphogenesis, proliferation and differentiation [8–11]. The adhesion and proliferation of different type of cells (include gingival fibroblasts) have previously been studied on various surfaces (e.g., on polystyrene, glass and titanium, hydroxyapatite/collagen composites) [12,13]. Many reports highlight the interaction between CNTs and different types of cells [14]. During *in vitro* studies, a good adhesion and proliferation of the investigated cells has been observed [15]. It has been found that CNTs combined with several materials (e.g., biopolymers) improve cell contact and adhesion [16]. CNT based nanomaterials allow for the quick adaptation of cells to a new environment by modulating the expression of a key protein involved in adhesion (integrin), as well as providing stronger adhesion and survival [17]. Aoki et al.

* Corresponding author.
** Corresponding author.
E-mail addresses: alicja@amu.edu.pl (A. Warowicka), bmacieje@amu.edu.pl (B.M. Maciejewska).
[1] These authors made equal contributions to the work.

http://dx.doi.org/10.1016/j.compscitech.2016.09.026
0266-3538/

reported osteoblast-like cell proliferation, showing that alkaline phosphatase activity and protein adsorption on CNT based substrates are higher than on polycarbonate membranes and graphite, as a result cell growth on CNTs greatly extended in all directions [18]. Previous studies report that CNT based matrices can be also applied to enhance the growth and differentiation of neurons [19]. One of approaches is to use MWCNT based structures as scaffolds for tissue engineering, for example potential biomaterial in bone reconstruction. It has been shown that carbon nanotube composite scaffolds are biocompatible materials with sufficient mechanical strength for the repair and regeneration of bone [20]. Different groups of nanomaterials can be considered in term of using them in biomedical applications i.e. individual CNTs, CNTs filled with magnetic nanoparticles, CNT based carpets. Due to their unique physical, chemical and mechanical properties as well as the possibility of their biofunctionalization, CNTs can be potentially applied in drug delivery systems, bio-imaging, contrast agents, gene carriers and as implants [21–23]. However, the surface modification and cytotoxicity of carbon nanomaterials are a crucial points in case of cell adhesion, therefore biocompatibility control. In the scientific literature there is still many contradictory results about cytotoxicity of CNTs [24]. In recent years, CNT carpets have gained attention in *in vitro* studies due to their high processing capability, mechanical stability, low cytotoxicity and parallel alignment [25]. Due to their potential application for tissue engineering, it is important to study the cell adhesion and growth on different sorts of MWCNT matrices, i.e. pristine MWCNT based carpers or covalently modified. Well-aligned MWCNT based matrices, i.e. MWCNT carpets, enable them to be used in regenerative medicine and tissue engineering [26]. The distribution of functionalized MWCNTs in the scaffold structures enhances surface hydrophilicity and provides a preferable microenvironment for cell attachment [27]. Mainly, MWCNT based carpets are synthesized by the Floating Catalyst Chemical Vapor Deposition (FCCVD) route on a quartz substrate typically using a metallocene-hydrocarbon solution [28]. This method allows control over the size, shape and alignment of MWCNT based matrices. In recent years, scientists have drawn attention to the application of carbon materials in dentistry and oral regenerative medicine, thus composites are more tough and can be easily employed as implants. Since MWCNTs might be produced in different forms, they can be used as a new class of implants. Previous research has concluded that CNT functionalized with sodium hyaluronate (HY-SWCNT) may be a potential biomaterial for application in dentistry in regenerative therapies, i.e. for tooth socket repair [29]. Dental filling (glass ionomer cement) with incorporated MWCNTs for dental restorations has revealed high strength and hardness and reduced loss due to friction and wear [30]. Due to the increasing attention of MWCNT based matrices in dentistry and tissue engineering, it is necessary to study various cellular mechanisms, for example adhesion and proliferation.

In this work, we synthesized, modified and characterized the surface of MWCNT based carpets in terms of their potential usefulness in cell culturing and tissue engineering. Annealing at 1900 °C, purification in hydrochloric acid (HCl) and oxidation in Sulfuric and Nitric acid were conducted in order to change the MWCNT morphology and surface. We investigated the effect of MWCNTs on the viability of human gingival fibroblast (HGF-1) and human bone osteosarcoma epithelial (U2OS) cell lines. Furthermore, we studied the interaction of cells with the potential scaffolds by using Scanning Electron Microscopy, Atomic Force Microscopy and Confocal Microscopy. We have found that the F-actin cytoskeleton organization modulates the MWCNT matrices surface. We also discussed their capability for future orthopedics and dental implants as well as tissue engineered scaffolds.

2. Materials and methods

2.1. MWCNT carpet synthesis

Multiwall carbon nanotube based carpets were synthesized by using the Floating Catalyst Chemical Vapor Deposition (FCCVD) route. Ferrocene was used as a catalyst and toluene as a carbon source, as a result, well-aligned MWCNT carpets were obtained (as-prepared denoted as AP-MWCNT) [31]. Two sorts of MWCNT based carpets with 2 wt%, 5 wt% of ferrocene were used for further investigations. The ferrocene concentration determined the diameter of MWCNTs and the Fe particles size embedded within the tube. MWCNT carpets were annealed for two hours in argon atmosphere at 1900 °C to obtain well-graphitized MWCNT carpets (AN-MWCNT) and to remove the Fe particles from the MWCNTs. Furthermore, all carpets were treated with HCl at 60 °C overnight to obtain purified MWCNT (HCl-MWCNT). Finally, to attach covalently functional groups to the outer surface of MWCNTs, reflux treatment was conducted at 120 °C for 20 min using a sulfuric/nitric acid mixture (sulfuric acid 98% and nitric acid 70%, Sigma–Aldrich) – REF-MWCNT. Multiwall carbon nanotube based carpets (5%) were milled for 10 h in a quartz container using the Retsch MM40 mill in order to obtain fine MWCNT powder.

2.2. Structural and morphological characterization

The morphology of MWCNT based carpets was studied under a Scanning Electron Microscope (SEM Jeol 7001TTLS). The Raman spectroscopy data were obtained on a inVia Ranishaw confocal Raman microscope (Ranishaw) with 50 × /0.75 microscope objective (LEICA) and by engaging 633 nm He/Ne laser with 1800 gr mm^{-1} grating. The laser power used was 1.5 mW at the stage. All experiments were done on the powdered samples. Each Raman spectrum was obtained in the range of 1000–3000 cm^{-1} corrected by the WiRE™ 3.3 software attached to the instrument.

Fourier Transformed Infrared (FTIR) absorption spectra were obtained using a Bruker Optics IFS 66/s spectrometer in the wave number range 800 cm^{-1} to 4500 cm^{-1} with a resolution of 4 cm^{-1}. Pre-measured carbon structures were mixed with potassium bromide (KBr) and then compressed into a thin pallet. Thermal Gravimetric Analysis (TGA) was carried out in air atmosphere by heating the samples up to 1000 °C at a rate of 10 °C/min. Atomic force microscopy (AFM) measurements were performed using the Icon Scanning Probe Microscope (Bruker) in contact mode. Antimony doped silicon tips (RTESP, f_0: 339–352 kHz k: 20–80 N/m) were used for MWCNT carpets imaging. Each topography image was obtained at 0.2 Hz and 512 lines. All AFM data analysis were performed by Gwyddion software.

2.3. Cell culture

Human bone osteosarcoma (U2OS) cell line and human gingival fibroblasts (HGF-1) cell line were purchased from the American Type Culture Collection (ATCC, USA). U2OS cells were cultured in Dulbecco's Modified Eagle Medium (DMEM, Sigma–Aldrich) supplemented with 10% (v/v) fetal bovine serum (FBS, Sigma–Aldrich) and 1% (v/v) antibiotics (penicillin, streptomycin). HGF-1 cells were grown in Dulbecco's Modified Eagle Medium (DMEM, ATCC) modified to contain 1 mM sodium pyruvate and supplemented with 10% (v/v) fetal bovine serum (FBS, Sigma–Aldrich). Cells were grown as a monolayer at 37 °C under a humidified atmosphere of 5% CO_2. When the culture reached a near confluence 80%, cells were washed with phosphate buffer saline (PBS), trypsinized with Trypsin-EDTA (Sigma–Aldrich), counted using an Automated Cell Counter (BioRad) and passaged on sterile tissue culture plates.

2.4. Cell imaging by SEM

SEM analyses were used to study cell attachment to the MWCNT based carpet surfaces. U2OS and fibroblasts cells were seeded at a cell concentration of 1×10^4 cells/mL onto the MWCNT based carpets and incubated for 24 h. All MWCNT based carpets were sterilized prior cell seeding using UV irradiation (UVc, ~254 nm). Sterile MicroWell Plates (HydroCell, Thermo Scientific) were used to prevent cells from attaching to the well surfaces. The adhesion of U2OS cells was analyzed by SEM after fixing with glutaraldehyde (2.5%) in PBS and cacodylate buffer 0.1 M (cacodylic acid, Sigma–Aldrich), dehydrating with a graded series of ethanol (50%, 75%, 90% and 100%) for 10 min each. Then, samples were coated with 100 nm Au layer prior to SEM imaging at an accelerating voltage of 5 kV. The adhesion of cells on MWCNT based carpets was analyzed using a JEOL scanning electron microscope (SEM Jeol 7001TTLS).

2.5. Cell imaging by confocal microscopy

To assess the cytoskeletal responses (organization) of gingival fibroblasts to the MWCNT based carpets confocal microscopy was applied. Oregon Green 488 Phalloidin (Life Technologies) and DRAQ5 (Cell Signaling Technology) dyes were used to stain the cytoskeleton and nuclei, respectively. HGF-1 cells (1×10^4 cells/well) were seeded onto the MWCNT based carpets using an 8-well LabTek chambered cover-glass system (Nunc) and cultivated for 24 h. Then, the samples were processed for confocal microscopy visualization. Before Oregon Green 488 Phalloidin staining, MWCNT based carpets were washed twice with PBS (Sigma–Aldrich) to remove non-adherent cells. Then, the samples were fixed with 3.7% (v/v) formaldehyde solution (Sigma–Aldrich) in PBS and then permeabilized 0.1% (v/v) Triton X-100 (Sigma–Aldrich) in PBS for 5 min. Oregon Green 488 Phalloidin solution in PBS containing 1% BSA was added to each well and then incubated for 20 min at room temperature. After incubation, samples were washed twice in PBS. Cell nuclei were stained with DRAQ5 at a concentration of 5 μM for 5 min at room temperature. Finally, samples were washed twice with PBS and immediately observed using confocal microscopy. Samples were visualized with an Olympus FV 1000 confocal microscope. The 488 nm (for Oregon Green) and 635 nm (for DRAQ5) line lasers were used for fluorescence excitation of HGF-1 cell organelles and the emitted light was detected in the range of 495–580 nm and 655–755 nm, respectively.

2.6. Cell viability and cytotoxicity analyses

The cell viability after incubation with MWCNTs was evaluated using Cell Proliferation Reagent WST-1 (Clontech) and Cell Counting Kit-8 CCK-8 (Sigma). U2OS and fibroblast cells were plated in 96-well plates with density of 1×10^4 cells per well and incubated for 24 h in 37 °C, 5% CO_2 atmosphere. After incubation overnight, the medium was removed and several concentrations (6, 10, 30, 50, 100, 200, 300, 500, 600 μg/mL) of MWCNT powder dispersed in cell medium were added to the cells. Cells cultured without MWCNTs were used as the positive control. Wells which were treated with DMSO (10% - dimethyl sulfoxide) represented the negative control. After 24 h, 10 μL of WST-1 and CCK-8 solution was added to each well and incubated for an additional 1, 2 and 3 h at 37 °C. The optical density of each well was determined at 450 nm by using spectrophotometrically multiwall plate reader (Biochrom Anthos Zenyth 340). Each experiment was repeated three times.

2.7. RNA extractions and cDNA synthesis

The U2OS cells were seeded at a density 1.5×10^5 cells/ml on MWCNTs based carpets and maintained for 24 h in an incubator under standard conditions (at 37 °C, humidified atmosphere of 5% CO_2). As well, HGF-1 and U2OS cells were cultivated separately with MWCNTs (10 μg/ml and 30 μg/ml) that were used for carpet synthesis.

Total RNA from cells was extracted by using RNeasy Mini Kit (Qiagen) according to the manufacturer's protocols. The purity and concentration of obtained RNA were determined spectrophotometrically by NanoDrop 2000c (Thermo Scientific). For each sample, 1 μg of RNA was used for reverse transcriptase reaction (cDNA synthesis) by using QuantiTect Reverse Transcription Kit (Qiagen). Each reaction of cDNA synthesis was carried out in 14 μl volume. The reactions were carried out according to the QuantiTect Reverse Transcription Kit (Qiagen) suggested manual. In next step, the synthetized cDNA was used for real time PCR experiments.

2.8. Measurement of cell adhesion relative–gene expression level by qRT-PCR

In this study we analyzed the expression of the adhesion related genes using quantitative Real time PCR (qRT-PCR) technique. The qRT-PCR experiments were performed on a CFX96 (C1000) (Bio-Rad) instrument in 96-well plates (Multiplate PCR Plates, Low 96-well Clear, Bio-Rad). In this work we monitored the number of mRNA copies for integrin, vinculin, talin, fibronectin, osteonectin and GAPDH (human glyceraldehyde-3-phosphate dehydrogenase) used as a housekeeping reference gene. Each qRT-PCR reaction mixture consisted of cDNA template, SYBR Green dye (iTaq Universal SYBR Green Supermix, Bio-Rad), forward and reverse primers, sterile DNase-free water (Sigma). The total volume of each reaction was 10 μl. All reactions were performed in triplicate. Primers sequences and thermal profile of qRT-PCR reactions are listed in Supplementary materials.

3. Results and discussion

3.1. Morphological characterization

The hydrophobic MWCNT matrixes (Fig. 1a) were firstly characterized by SEM (Fig. 1b). Consecutively, the quality of the investigated MWCNT carpets was assessed quantitatively by Raman Spectroscopy. The Raman spectra of 5% AP-MWCNTs, AN-MWCNTs, HCl-MWCNTs and REF-MWCNTs are presented in Fig. 1c. The AP-MWCNTs show the characteristic modes: D (double-resonance mode), G (tangential stretching mode), G′ (two phonon process) at 1338 cm^{-1}, 1586 cm^{-1}, 2665 cm^{-1}, respectively. Annealing and further purification of the carpets cause a shifting of peak positions to a lower wave number. The D-band is indicative of structural disorder due to disruption of sp^2 C=C bonds, whereas the G-band results come from the tangential vibration of graphitic carbon atoms [32]. The ratio of integral intensities $I_{D/G}$ commonly used for a quantitative estimation of the defect density and amount of amorphous carbon on the MWCNT walls is 0.95 for AP-MWCNTs (see Fig. 1d) and this decreases for AN-MWCNTs and HCl-MWCNTs to 0.62 and 0.61, respectively. During the oxidation process, the graphite-like structure of the MWCNT walls is damaged but in a controllable manner and the functional groups are attached to their surface. This is reflected in the increase in the $I_{D/G}$ for REF-MWCNTs ($I_{D/G}$ = 0.85) compared with AN-MWCNTs and HCl-MWCNTs. Mode G′ is particularly sensitive to sample purity [33]. It is evident in Fig. 1d that the largest treatment dependent change is observed for the intensity ratio $I_{G'/D}$.

Owing to its high sensitivity to the localized vibration of molecular moieties, FTIR spectroscopy is a perfect tool to identify molecular groups attached to the MWCNT walls. Fig. 2a shows infrared spectra of 5%-MWCNTs for as-prepared, annealed, purified

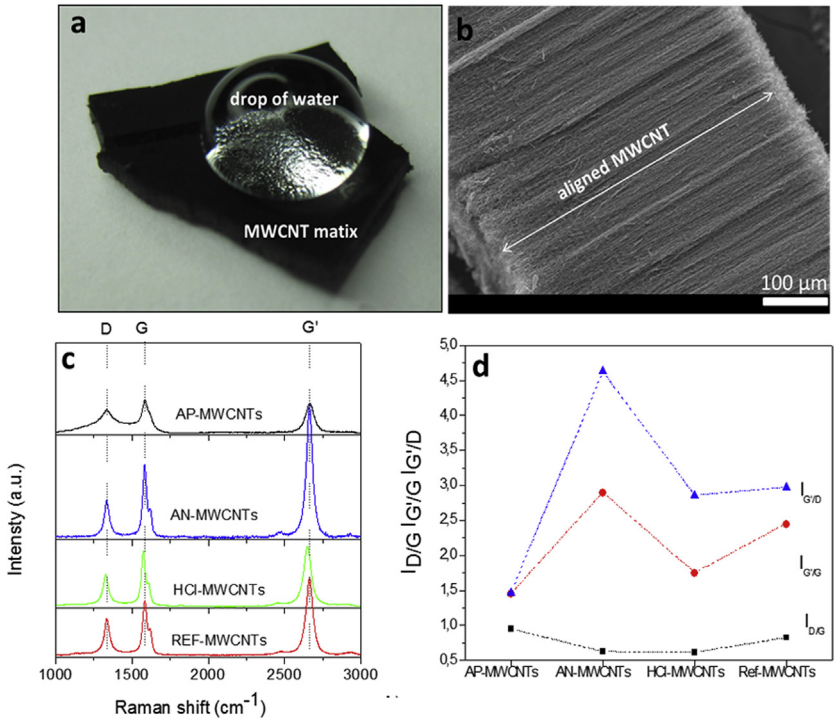

Fig. 1. a) Picture of hydrophobic MWCNT carpet and b) SEM micrograph of aligned MWCNTs. c) Raman spectra of 5% AP-MWCNTs, AN-MWCNTs, HCl-MWCNTs and REF-MWCNTs. d) Three different ratios of D, G, G′ Raman peaks for selected samples.

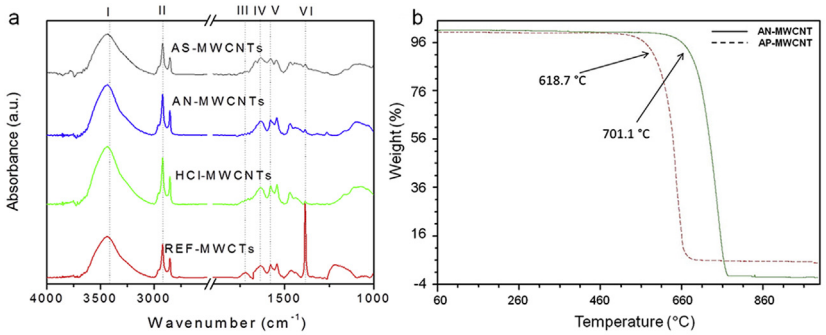

Fig. 2. a) Infrared absorption spectra of 5% AP-MWCNT, AN-MWCNT, HCl- MWCNT and REF-MWCNT carpets. The Roman numerals denote the following vibrations: (I) OH stretching, (II) CH_3 symmetric and asymmetric stretching, (III) C═O stretching, (IV, V) C═C stretching of aromatic groups of CNTs, (VI) CH bending vibration in COH moieties. b) Thermal Gravimetric analysis for 5% AP-MWCNTs and AN-MWCNTs.

and refluxed samples. Absorption peaks at IV (at 1635 cm^{-1}) and V (1570 cm^{-1}), corresponding to the C═C stretching mode of the aromatic core within CNTs, are more pronounced for purified carpets than as-synthesized ones. During the oxidation treatment, carboxyl and aldehyde groups are created. Consequently, peak III (at 1720 cm^{-1}) attributed to C═O stretching vibration within the carboxyl group and the absorption band (at 1380 cm^{-1}) ascribed to CH vibration in COH group show up in the spectrum of the refluxed sample [34]. The impact of the MWCNT diameter and length on the efficiency of the oxidation process is described elsewhere [31].

To study the thermal stability, thus the quality of the MWCNT based material, thermal analysis was performed. The purity of the carbon based materials, i.e. amorphous carbon species and embedded Fe particles within MWCNTs, was examined as well. Apart from the initiation temperature, in which the material starts to decompose, a highly valuable parameter is the so-called oxidation temperature, which is often described as the thermal stability point of a carbon based material. The more graphitized the carbon based material, the higher the thermal stability point is [35,36]. Fig. 2b shows the weight loss vs temperature dependency for both AP-MWCNT and AN-MWCNT. The initiation temperature was around 618.7 °C and 701.1 °C for AP-MWCNT and AN-MWCNT, respectively. Additionally, the oxidation temperature was much higher for MWCNTs after the annealing process compared to as-prepared ones. This confirms the higher quality of the initial material used for further processing, i.e. fewer defects within the tubes or the presence of a catalyst. The properties of the samples were characterized using atomic force microscopy (AFM) working in contact mode in order to measure the roughness of the samples (Fig. 3) which was found to be ≈ 600 nm.

3.2. MWCNT carpet – cell interaction studies by SEM and confocal microscopy

Cell attachments and morphology on differently modified MWCNT carpets were investigated using SEM and confocal

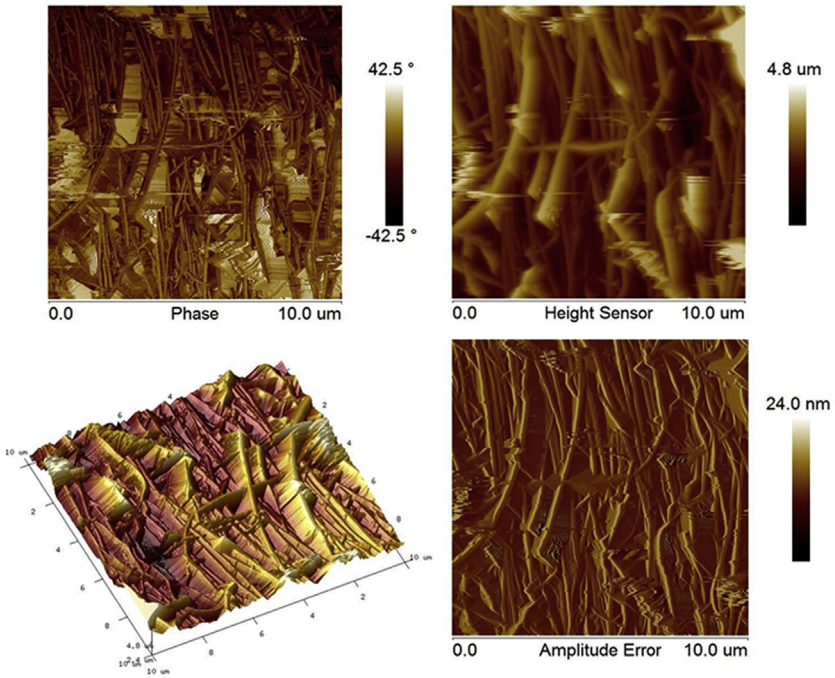

Fig. 3. AFM images of MWCNTs carpet.

microscopy. All carpets were verified in terms of their biocompatibility and possibility of use as potential scaffolds for two selected types of cell lines: HGF-1 and U2OS. In the field of biomaterials and its applications as scaffolds in tissue engineering, physical properties such as (elasticity, roughness) and chemical composition are essential and may modulate the condition of the cells. A good level of cells attachment to the MWCNT carpet was observed after one day of incubation (24 h). Moreover, the biocompatibility of MWCNT based carpets was increased by acid treatment. Considering the fact that functionalized (REF-MWCNTs) are more hydrophilic, cell interactions may be better than those for non-functionalized ones, i.e. AP-MWCNT, AN-MWCNT, HCl-MWCNT. In addition, MWCNT based carpets changed their structure after acid treatment (Fig. 4) and SEM analysis confirmed cell anchoring after the incubation of cells with both 2% REF-MWCNT (see Supplementary materials) and 5% REF-MWCNT. As shown in Fig. 4 a,b, the HGF-1 cells were elongated

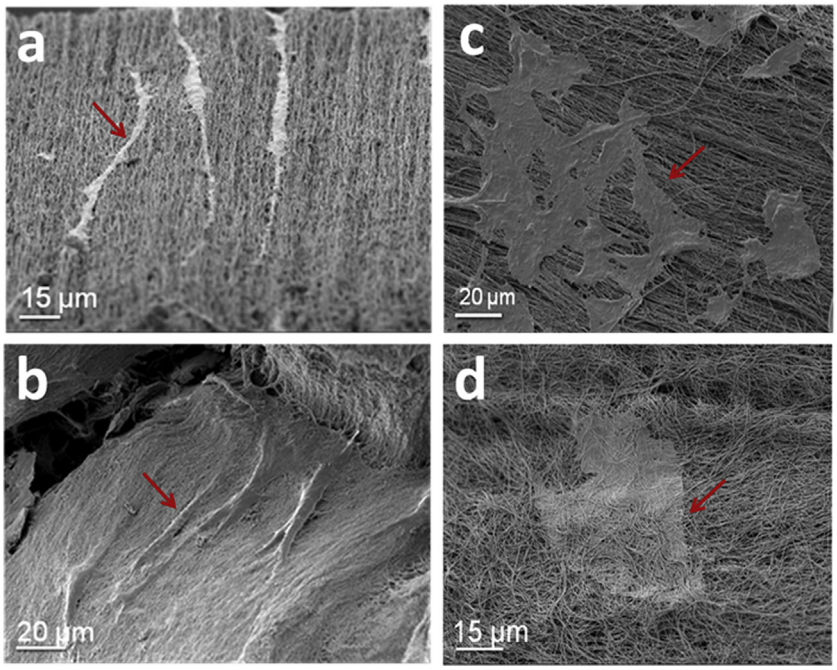

Fig. 4. SEM images of HGF-1 and U2OS cells grown on 5% MWCNT carpets after 24 h of incubation. a) HGF-1 cells on 5% HCL-MWCNT, b) HGF-1 cells on 5% REF-MWCNT, c) U2OS cells on 5% HCL-MWCNT, d) U2OS cells on 5% REF-MWCNT. Arrows indicate cells on the MWCNT matrices surface.

along MWCNTs on the side of 5% REF-MWCNTs carpet. Similarly, in Fig. 4c,d, U2OS cells were well adhered to the 5% REF-MWCNTs matrices.

Additionally, cell imaging via a confocal microscope was investigated in order to observe the morphology and cell attachment on the scaffolds. The cytoskeleton structure was visualized after staining the samples with a high affinity F-actin Oregon Green 488 Phalloidin dye. Oregon Green provides green fluorescence, while phalloidin binds F-actin with high selectivity. Additionally, nuclei were stained with DRAQ5 dye. The cytoskeleton of cells growing on a MWCNT carpet is clearly visible and this indicates the normal growth and proliferation of the cells. However, the shape and roughness of the top walls of the scaffold surfaces induce the reorganization of the actin cytoskeleton. The confocal microscopy imaging shows the loss of the typical elongated morphology and cytoskeleton organization of the HGF-1 cells (Fig. 5b and c). The actin filament network spreads in different directions modifying the proper organization and location of F-actin. In control samples (cells incubated in LabTek chamber cover glass system), the cytoskeleton arrangement tends to be aligned in one direction (Fig. 5f and g). Nucleus morphology investigation revealed an unchanged shape and size for cells grown on MWCNT matrices, thus that the incubation of cells with MWCNT matrices does not induce cell death. We conclude that the oxidized surface on MWCNT (REF-MWCNT) enables the creation of good environmental conditions for cells to grow and proliferate.

Another factor which can improve cell adhesion is protein serum, which penetrates through MWCNT matrix pores. MWCNT carpets can easily be permeated by proteins and growth factors present in the culture medium. A similar feature has already been observed by He et al. [37] for NIH 3T3 cells. The obtained results suggest that MWCNT carpets investigated in this study can be considered to be three dimensional (3D) scaffolds. Fig. 6 shows the SEM images of HGF-1 cells cultured with an HCl-MWCNT carpet which confirms that gingival fibroblasts are attached to the edges, sides and top surfaces of matrices. Confocal images (Fig. 6) of nuclei and cytoskeleton after DRAQ5 staining verify the possibility of cell growth along the sides of carpets.

In order to verify the possibility of applying MWCNT based carpets as scaffolds, another type of cells was tested in this study. Similar to HGF-1, U20S cells were well distributed on carpet surfaces, especially in the case of HCl-MWCNT matrices. In contrast to HGF-1, we noticed that U2OS cells create homogenous films, preferentially on HCl-MWCNT (Fig. 4c). Therefore, cells also migrate inside the carpets and grow towards the MWCNT matrices for REF-MWCNT (Fig. 4d).

Interestingly, the cells show close contacts with the surrounding MWCNTs within carpets. A number of filopodia were found after cell incubation with both HCl-MWCNT and REF-MWCNT carpets. The strong attachment between fibroblast HGF-1 cells and MWCNTs within the matrices suggests the low toxicity of potential scaffolds. SEM analysis showed the formation of tight junctions between cell filopodia and MWCNTs (Fig. 7). These results confirm the biocompatibility of the studied materials. Based on many scientific data and our studied carbon platform can be potentially used as a scaffold materials [38,39].

3.3. Cytotoxicity

The cell viability was determined to estimate the toxicity of MWCNTs using the WST-1 and CCK-8 assays. In both tests the formation of formazan dye depends on the mitochondrial activity. To evaluate MWCNTs cytotoxicity, U2OS and fibroblast cells were treated for 24 h with several concentrations of MWCNT in humidified atmosphere. Two controls were designed, negative untreated control which was the maximum cells viability (97–99%) and positive control in which was the cells were treated with DMSO (9–24%). The WST-1 and CCK-8 assays results of Fig. 8 demonstrates a prominent decrease metabolic activity of cells treated increasing concentrations of MWCNTs. Using a concentration of 600 μg/mL resulted in a survival rate of 55% in U2OS and 21% in HGF-1 for WST-1 assay, and properly 49% and 29% for CCK-8 assay. Studied concentrations of MWCNTs did not show the significant cytotoxicity (Fig. 8).

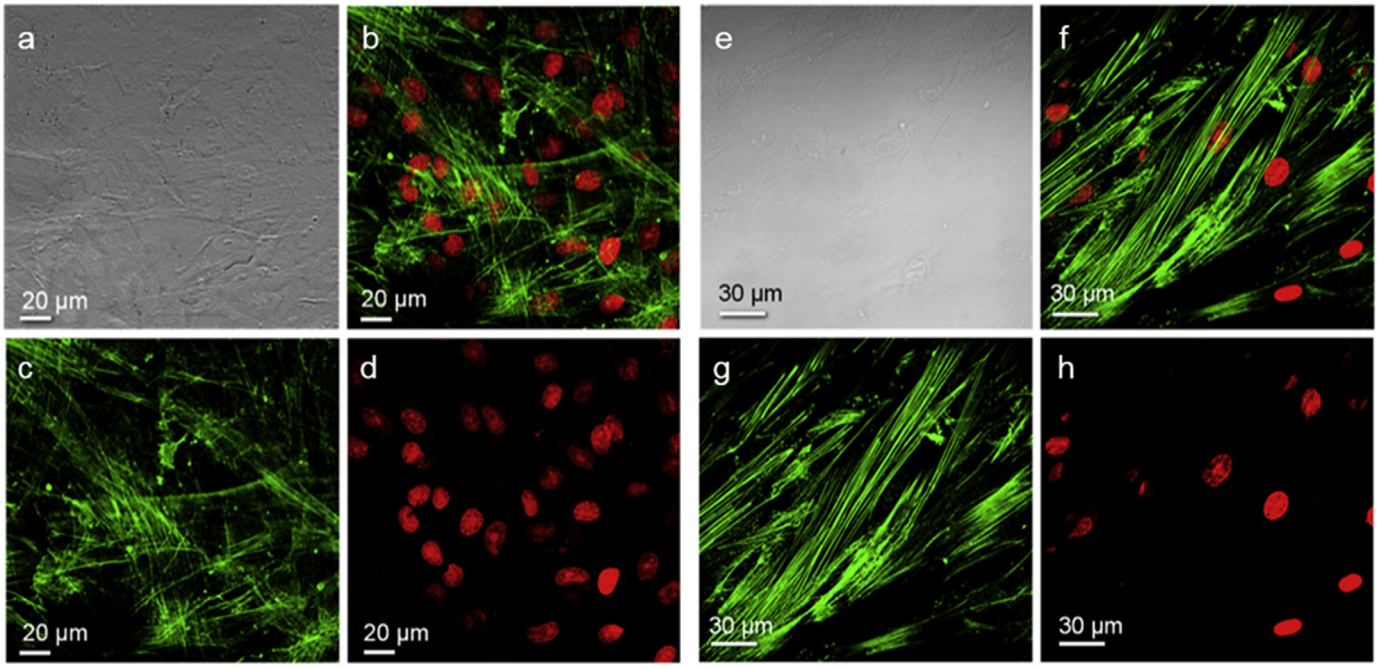

Fig. 5. Confocal images of HGF-1 grown on (a–d) 5% HCl-MWCNT carpets and (e–h) wells (cells incubated in LabTek chamber cover glass) after cytoskeleton and nuclei staining.

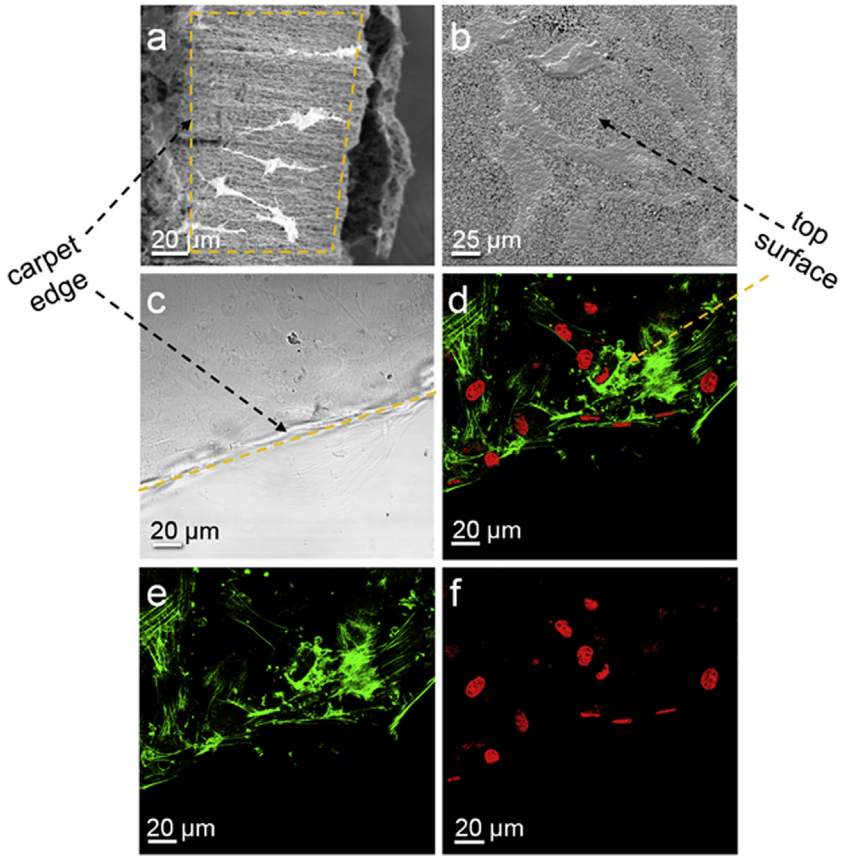

Fig. 6. HGF-1 cells on 5% HCl-MWCNTs; a,b) SEM images and c–f) confocal images after cytoskeleton and nuclei staining of cells on HCl-MWCNT carpets. On a and c dashed arrows indicate the carpet edges. b and d show the top surfaces of a carpet.

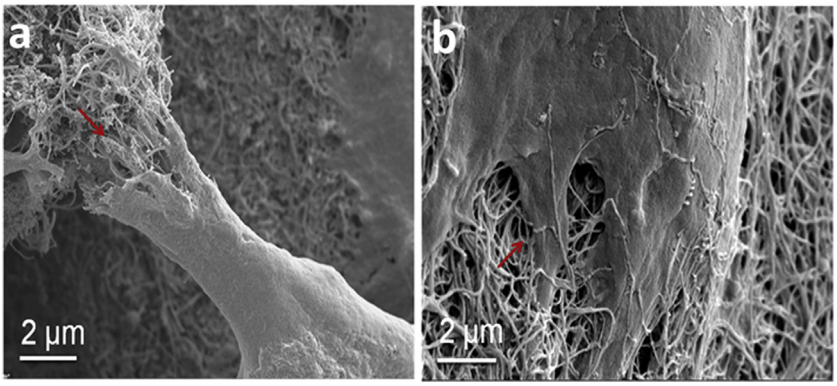

Fig. 7. SEM images of contacts between HGF-1 cells and MWCNTs; a, b) HCl-MWCNT and c, d) REF-MWCNT. Red arrows point tight junctions between cell filopodia and MWCNTs. (For interpretation of the references to colour in this figure legend, the reader is referred to the web version of this article.)

3.4. Quantitative RT-PCR (qRT-PCR)

The expression (the number of mRNA copies) of the adhesion related genes was determined in samples taken from U2OS cells incubated for 24 h on MWCNT based carpets as well as with O-MWCNT (after REF treatment) powder. Similarly, the mRNA level for the adhesion related genes was studied for HGF-1 cells incubated for 24 h with O-MWCNTs. The number of transcript copies was normalized to GAPDH expression level. The higher gene expression level was obtained for integrin, talin and fibrinectin in U2OS cells grown on MWCNTs carpets compared with cells incubated on control substrate (tissue plate). Integrins play a significant role in cell adhesion, invasion and migration. Those cell receptors allow the attachment of cells to their surrounding environment e.g. extracellular matrix or other cells. Moreover, are essential for transmission of intracellular signals that regulate cell adhesion process [40]. In our research we noticed the higher expression level of integrin, fibronectin and talin for U2OS cells cultivated on MWCNT carpets. Conversely, we observed the lower expression level of integrin and fibronectin for HGF-1 after incubation with MWCNTs. We attribute these changes to the expression level of fibronectin which is related to expression level of integrin into the cell and its influence on the modification of cell cytoskeleton organization and cell adhesion to MWCNT carpets. Differences

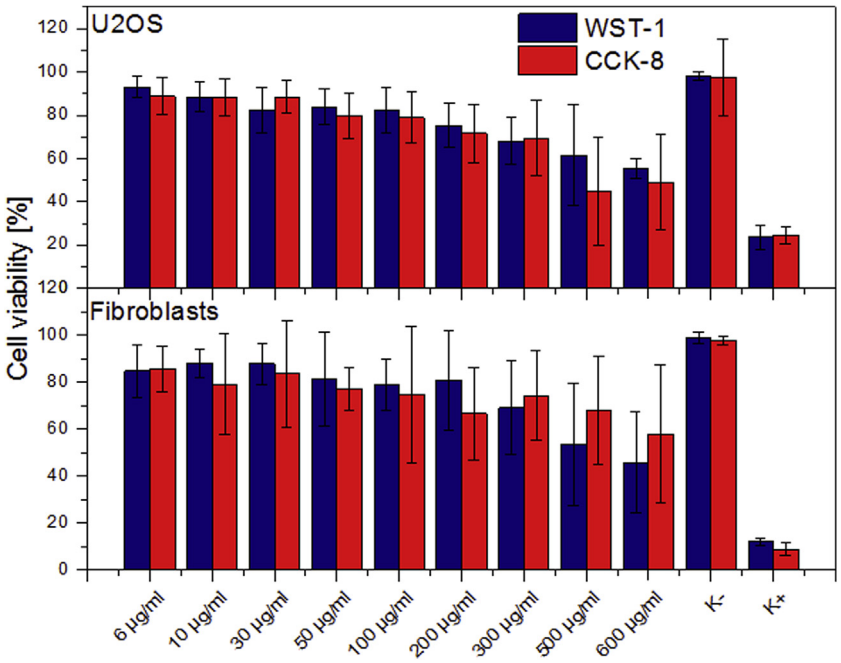

Fig. 8. Cell viability obtained for (a) U2OS and (b) Fibroblast cell lines for various concentration of MWCNT. Relative cell viability was determined by WST-1 and CCK-8 assays. Data are shown as means of four independent experiments with standard deviations. K^- are untreated cells and K^+ cells treated with DMSO.

between fibronectin level of U2OS and HGR-1 results from different type of studied cell lines i.e. osteosarcoma and normal fibroblasts.

In our studies we noticed increase of gene expression for talin in HGF-1 cells cultured on O-MWCNTs (30 μg/ml) compared with cells incubated with O-MWCNTs (10 μg/ml) and grown on control substrate. Interestingly, U2OS cultured on carpets and MWCNTs as well as HGF-1 cells grown with MWCNTs showed decreased expression level of vinculin and osteonectin (Fig. 9). Vinculin is a protein with many binding site for cytoskeletal proteins and plays role in the initial contact between cells and the extracellular matrix. Similarly, in previous studies, Soo-Ryoon et al. showed significantly lower expression of vinculin in NIH-3T3 fibroblasts after 24 h of incubation with reduced graphene oxide and MWCNTs [41].

4. Conclusion

The structural analysis revealed that modified MWCNT matrices have better quality than as-prepared ones. The high roughness

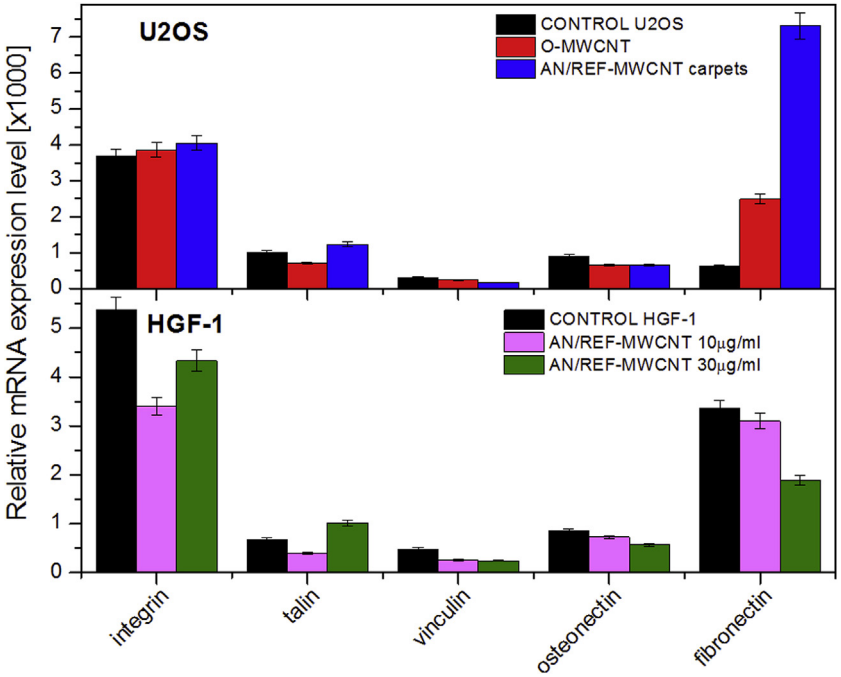

Fig. 9. Expression profile of adhesion related genes (integrin, talin, vinculin, osteonectin and fibronectin) for U2OS and HGF-1 cells for MWCNT carpets and oxidized (REF) MWCNT powder respectively.

factor of side walls of MWCNT carpets enables the cell attachment. Moreover, to obtain high hydrophilic and biocompatible surfaces, MWCNT carpets were defected in a controllable manner. The existence of carboxyl and aldehyde groups resulted in evident attachment of HGF-1 and U2OS cells for purified and oxidized samples. The F-actin cytoskeleton organization indicated cell growth in different directions on the matrix top surfaces. Additionally, the proper cell adhesion is confirmed by the increase of expression level of selected adhesion related genes (talin, integrin and fibronectin for U2OS). Rapid decrease of viability for U2OS and fibroblast cells was not observed. Our research showed that MWCNT based carpets are biocompatible with human bone osteosarcoma cells and gingival human fibroblasts, clearly showing that these materials may be used as matrices for future potential tissue engineering applications.

Acknowledgements

Authors gratefully acknowledge to Dr Emerson L. Coy for his advices and critical reading of the manuscript. Financial support from the National Centre for Research and Development under research grant “Nano-materials and Their Application to Biomedicine”, Contract PBS1/A9/13/2012, National Science Centre (UMO-2013/11/D/ST5/02900) as well as OPUS 6 (UMO-2013/11/B/ST3/04190).

Appendix A. Supplementary data

Supplementary data related to this article can be found at http://dx.doi.org/10.1016/j.compscitech.2016.09.026.

References

[1] L. Yate, L.E. Coy, D. Gregurec, W. Aperador, S.E. Moya, G. Wang, Nb-C nanocomposite films with enhanced biocompatibility and mechanical properties for hard-tissue implant applications, ACS Appl. Mater. Interfaces 7 (2015) 6351–6358, http://dx.doi.org/10.1021/acsami.5b01193.
[2] M.C. Serrano, M.C. Gutiérrez, F. Monte, Progress in Polymer Science Role of polymers in the design of 3D carbon nanotube-based scaffolds for biomedical applications, Prog. Polym. Sci. 39 (2014) 1448–1471, http://dx.doi.org/10.1016/j.progpolymsci.2014.02.004.
[3] T. Dvir, B.P. Timko, D.S. Kohane, R. Langer, Nanotechnological strategies for engineering complex tissues, Nat. Nanotechnol. 6 (2011) 13–22, http://dx.doi.org/10.1038/nnano.2010.246.
[4] P.E. Mikael, A.R. Amini, J. Basu, M. Josefina Arellano-Jimenez, C.T. Laurencin, M.M. Sanders, et al., Functionalized carbon nanotube reinforced scaffolds for bone regenerative engineering: fabrication, in vitro and in vivo evaluation, Biomed. Mater. Bristol Engl. 9 (2014) 035001, http://dx.doi.org/10.1088/1748-6041/9/3/035001.
[5] N. Saito, Y. Usui, K. Aoki, N. Narita, M. Shimizu, N. Ogiwara, et al., Carbon nanotubes for biomaterials in contact with bone, Curr. Med. Chem. 15 (2008) 523–527, http://dx.doi.org/10.2174/092986708783503140.
[6] S. Namgung, T. Kim, K.Y. Baik, M. Lee, J.-M. Nam, S. Hong, Fibronectin-carbon-nanotube hybrid nanostructures for controlled cell growth, Small 7 (2011) 56–61, http://dx.doi.org/10.1002/smll.201001513 (Weinheim an Der Bergstrasse, Germany).
[7] J.-R. Lee, S. Ryu, S. Kim, B.-S. Kim, Behaviors of stem cells on carbon nanotube, Biomater. Res. 19 (2015) 3, http://dx.doi.org/10.1186/s40824-014-0024-9.
[8] E. Hirata, C. Ménard-Moyon, E. Venturelli, H. Takita, F. Watari, A. Bianco, et al., Carbon nanotubes functionalized with fibroblast growth factor accelerate proliferation of bone marrow-derived stromal cells and bone formation, Nanotechnology 24 (2013) 435101, http://dx.doi.org/10.1088/0957-4484/24/43/435101.
[9] E.W. Brunner, I. Jurewicz, E. Heister, A. Fahimi, C. Bo, R.P. Sear, et al., Growth and proliferation of human embryonic stem cells on fully synthetic scaffolds based on carbon nanotubes, ACS Appl. Mater. Interfaces 6 (2014) 2598–2603, http://dx.doi.org/10.1021/am405097w.
[10] Z. Jun Han, A.E. Rider, M. Ishaq, S. Kumar, A. Kondyurin, M.M.M. Bilek, et al., Carbon nanostructures for hard tissue engineering, RSC Adv. 3 (2013) 11058, http://dx.doi.org/10.1039/c2ra23306a.
[11] E. Mooney, P. Dockery, U. Greiser, M. Murphy, V. Barron, Carbon nanotubes and mesenchymal stem cells: biocompatibility, proliferation and differentiation, Nano Lett. 8 (2008) 2137–2143, http://dx.doi.org/10.1021/nl073300o.
[12] S. Lavenus, P. Pilet, J. Guicheux, P. Weiss, G. Louarn, P. Layrolle, Behaviour of mesenchymal stem cells, fibroblasts and osteoblasts on smooth surfaces, Acta Biomater. 7 (2011) 1525–1534, http://dx.doi.org/10.1016/j.actbio.2010.12.033.
[13] D.M. Veríssimo, R.F.C. Leitão, R.A. Ribeiro, S.D. Figueiró, A.S.B. Sombra, J.C. Góes, et al., Polyanionic collagen membranes for guided tissue regeneration: effect of progressive glutaraldehyde cross-linking on biocompatibility and degradation, Acta Biomater. 6 (2010) 4011–4018, http://dx.doi.org/10.1016/j.actbio.2010.04.012.
[14] X. Zhang, X. Wang, Q. Lu, C. Fu, Influence of carbon nanotube scaffolds on human cervical carcinoma HeLa cell viability and focal adhesion kinase expression, Carbon 46 (2008) 453–460, http://dx.doi.org/10.1016/j.carbon.2007.12.015.
[15] S.L. Edwards, J.S. Church, J.A. Werkmeister, J.A.M. Ramshaw, Tubular microscale multiwalled carbon nanotube-based scaffolds for tissue engineering, Biomaterials 30 (2009) 1725–1731, http://dx.doi.org/10.1016/j.biomaterials.2008.12.031.
[16] C.Y. Tay, H. Gu, W.S. Leong, H. Yu, H.Q. Li, B.C. Heng, et al., Cellular behavior of human mesenchymal stem cells cultured on single-walled carbon nanotube film, Carbon 48 (2010) 1095–1104, http://dx.doi.org/10.1016/j.carbon.2009.11.031.
[17] A. Kroustalli, V. Kotsikoris, A. Karamitri, S. Topouzis, D. Deligianni, Mechanoresponses of human primary osteoblasts grown on carbon nanotubes, J. Biomed. Mater. Res. Part A (2014), http://dx.doi.org/10.1002/jbm.a.35250.
[18] N. Aoki, T. Akasaka, F. Watari, A. Yokoyama, Carbon nanotubes as scaffolds for cell culture and effect on cellular functions, Dent. Mater. J. 26 (2007) 178–185, http://dx.doi.org/10.4012/dmj.26.178.
[19] G.Z. Jin, M. Kim, U.S. Shin, H.W. Kim, Neurite outgrowth of dorsal root ganglia neurons is enhanced on aligned nanofibrous biopolymer scaffold with carbon nanotube coating, Neurosci. Lett. 501 (2011) 10–14, http://dx.doi.org/10.1016/j.neulet.2011.06.023.
[20] J. Venkatesan, B. Ryu, P.N. Sudha, S.-K. Kim, Preparation and characterization of chitosan-carbon nanotube scaffolds for bone tissue engineering, Int. J. Biol. Macromol. 50 (2012) 393–402, http://dx.doi.org/10.1016/j.ijbiomac.2011.12.032.
[21] S. Ostrovidov, X. Shi, L. Zhang, X. Liang, S.B. Kim, T. Fujie, et al., Myotube formation on gelatin nanofibers - multi-walled carbon nanotubes hybrid scaffolds, Biomaterials 35 (2014) 6268–6277, http://dx.doi.org/10.1016/j.biomaterials.2014.04.021.
[22] Y. Liu, T.C. Hughes, B.W. Muir, L.J. Waddington, T.R. Gengenbach, C.D. Easton, et al., Water-dispersible magnetic carbon nanotubes as T2-weighted MRI contrast agents, Biomaterials 35 (2014) 378–386, http://dx.doi.org/10.1016/j.biomaterials.2013.09.079.
[23] M. Zhu, G. Diao, Review on the progress in synthesis and application of magnetic carbon nanocomposites, Nanoscale 3 (2011) 2748–2767, http://dx.doi.org/10.1039/c1nr10165j.
[24] J.M. Wörle-Knirsch, K. Pulskamp, H.F. Krug, Oops they did it again! Carbon nanotubes hoax scientists in viability assays, Nano Lett. 6 (2006) 1261–1268, http://dx.doi.org/10.1021/nl060177c.
[25] B.S. Harrison, A. Atala, Carbon nanotube applications for tissue engineering, Biomaterials 28 (2007) 344–353, http://dx.doi.org/10.1016/j.biomaterials.2006.07.044.
[26] A. Abarrategi, M.C. Gutiérrez, C. Moreno-Vicente, M.J. Hortigüela, V. Ramos, J.L. López-Lacomba, et al., Multiwall carbon nanotube scaffolds for tissue engineering purposes, Biomaterials 29 (2008) 94–102, http://dx.doi.org/10.1016/j.biomaterials.2007.09.021.
[27] Y. Yang, S. Shi, Q. Ding, J. Chen, J. Peng, Y. Xu, Multiwalled carbon nanotube-modified poly(D,L-lactide-co-glycolide) scaffolds for dendritic cell load, J. Biomed. Mater. Res. Part A 103 (2015) 1045–1052, http://dx.doi.org/10.1002/jbm.a.35255.
[28] C. Singh, M. Shaffer, A. Windle, Production of controlled architectures of aligned carbon nanotubes by an injection chemical vapour deposition method, Carbon 41 (2003) 359–368.
[29] M.A. Sá, V.B. Andrade, R.M. Mendes, M.V. Caliari, L.O. Ladeira, E.E. Silva, et al., Carbon nanotubes functionalized with sodium hyaluronate restore bone repair in diabetic rat sockets, Oral Dis. 19 (2013) 484–493, http://dx.doi.org/10.1111/odi.12030.
[30] K.A. Bhat, R.N. Raghavan, D. Sangeetha, S. Ramesh, Multi-walled carbon nanotube reinforced glass ionomer cements for dental restorations, Trends Biomater. Artif. Organs 27 (2013) 168–176.
[31] B.M. Maciejewska, L.E. Coy, K.K.K. Koziol, S. Jurga, Facile synthesis of highly stable and water-soluble magnetic MWCNT/α-Fe nanocomposites, J. Phys. Chem. C 118 (2014) 27861–27869, http://dx.doi.org/10.1021/jp5077142.
[32] B.M. Maciejewska, M. Jasiurkowska-Delaporte, A.I. Vasylenko, K.K. Kozioł, S. Jurga, Experimental and theoretical studies on the mechanism for chemical oxidation of multiwalled carbon nanotubes, RSC Adv. 4 (2014) 28826, http://dx.doi.org/10.1039/c4ra03881a.
[33] M.S. Dresselhaus, G. Dresselhaus, R. Saito, A. Jorio, Raman spectroscopy of carbon nanotubes, Phys. Rep. 409 (2005) 47, http://dx.doi.org/10.1016/j.physrep.2004.10.006.
[34] G. Socrates, Infrared and Raman Characteristic Group Frequencies, Wiley-VCH Verlag GmbH & Co. KGaA, 2004, http://dx.doi.org/10.1002/jrs.1238.
[35] J.H. Lehman, M. Terrones, E. Mansfield, K.E. Hurst, V. Meunier, Evaluating the characteristics of multiwall carbon nanotubes, Carbon 49 (2011) 2581–2602, http://dx.doi.org/10.1016/j.carbon.2011.03.028.
[36] D. Bom, R. Andrews, D. Jacques, J. Anthony, B. Chen, M.S. Meier, et al., Thermogravimetric analysis of the oxidation of multiwalled carbon nanotubes:

evidence for the role of defect sites in carbon nanotube chemistry, Nano Lett. 2 (2002) 615–619, http://dx.doi.org/10.1021/nl020297u.
[37] L. He, P. Zhao, Q. Han, X. Wang, X. Cai, Y. Shi, et al., Surface modification of poly-l-lactic acid fibrous scaffolds by a molecular-designed multi-walled carbon nanotube multilayer for enhancing cell interactions, Carbon 56 (2013) 224–234, http://dx.doi.org/10.1016/j.carbon.2013.01.025.
[38] I. Jesion, M. Skibniewski, E. Skibniewska, W. Strupiński, L. Szulc-Dąbrowska, A. Krajewska, et al., Graphene and carbon nanocompounds: biofunctionalization and applications in tissue engineering, Biotechnol. Biotechnol. Equip. 29 (2015) 415–422, http://dx.doi.org/10.1080/13102818.2015.1009726.
[39] R. Baktur, S. Yoon, S. Kwon, Effects of multiwalled carbon nanotube reinforced collagen scaffolds on the osteogenic differentiation of mesenchymal stem cells, J. Nanomater. 2013 (2013) 1–9.
[40] J.D. Hood, D.A. Cheresh, Role of integrins in cell invasion and migration, Nat. Rev. Cancer 2 (2002) 91–100, http://dx.doi.org/10.1038/nrc727.
[41] S.R. Ryoo, Y.K. Kim, M.H. Kim, D.H. Min, Behaviors of NIH-3T3 fibroblasts on graphene/carbon nanotubes: proliferation, focal adhesion, and gene transfection studies, ACS Nano 4 (2010) 6587–6598, http://dx.doi.org/10.1021/nn1018279.